J. Univ. Kuwait (Sci) **20**, 1993

A study on the discretization and modelling errors of "STRUDL" in 3-D analysis

HANY A. EL-GHAZALY* AND MOSAID F. AL-HUSSAINI

Department of Civil Engineering, University of Kuwait, P.O. Box 5969, Safat 13060, Kuwait

ABSTRACT

Design of machinery or bulky structural components often necessitates the use of three dimensional (3-D) analysis. When using the finite element method (FEM) the first step is to select a suitable mesh to be used for the analysis. This study is about the effects of element aspect ratio and the type of element used on the accuracy of the solution. The well known "STRUDL" finite element package is used in this study in order to perform 3-D analysis where four elements from STRUDL element library were exclusively used. Three examples with known solution according to the theory of elasticity were employed in order to quantify the errors resulting from the application of the FEM. Attention is focused on 3-D discretization of long members where the dimension along the member axis is one order of magnitude higher than the cross-sectional dimensions. The conclusions drawn are limited to the applications solved; however, the study gives some idea about the order of magnitude of the errors involved in 3-D analysis for similar structures.

SYMBOLS

$[B]$ = strain-displacement matrix
$[\underline{B}]$ = strain-displacement differential operator matrix
b_i = body force vector (force/unit mass)
$[E]$ = elastic stress-strain matrix
e_σ = deviation of elemental nodal stress from smooth average stress
$[K]$ = system (structural) stiffness matrix
$[k]_e$ = element stiffness matrix
$\{N\}$ = shape functions vector
n_i = unit outward normal to the surface
$\{P\}$ = structural load vector
p_j = surface force per unit area
s = surface enclosing volume
s_p = portion of the surface with external traction forces
s_u = portion of the surface with prescribed displacement
s_{pe} = element surface area
$\{U\}$ = vector of structural nodal displacements
$\{u\}_e$ = element generalized nodal displacements
$\{\underline{u}\}$ = displacement vector field
$\{\underline{u}\}_e$ = assumed element displacement function

* Present address: Department of Civil Engineering, Faculty of Engineering, Fayoum, Egypt.

U^* = calculated strain energy of the system
u_i = linear displacement vector
u_i^p = prescribed displacement vector
v = volume of integration
v_e = element volume
δ_{ij} = Kronecker delta
$\{\delta \underline{u}\}$ = vector of admissible infinitesimal virtual displacement field
$\{\delta \underline{\varepsilon}\}$ = generated virtual displacement vector field
ε_{ij} = Lagrangian linear strain tensor
$\{\varepsilon\}$ = strain field
ν = Poisson's ratio (=0·3)
ρ = material density
$[\underline{\sigma}\}$ = stress field
σ_{ij} = stress tensor

INTRODUCTION

Errors and accuracy of stress analysis methods are a subject of paramount importance (Bubuska *et al.* 1986) since the design of the various structural and mechanical components depends largely on the results of the analysis. Needless to say that any refinement to the design methods becomes totally meaningless if the stresses are not accurately calculated.

The finite element method is presently the most popular numerical technique for the analysis of structures. The popularity of this method stems from its flexibility in representing virtually any loading and/or boundary conditions as well as its ability to handle a variety of material constitutive relationships. Presently, a user will find a variety of finite element packages for the analysis of structures, such as NASTRAN, ANSYS, MARC, or finite element-based programs for both analysis and design of structures such as STRUDL and STAADIII. Most of these packages are provided with powerful pre and post processors for efficient mesh generation and easy interpretation of results. Some of the recent versions of finite element packages (e.g. ANSYS) provide an estimate for the error of the solution based on the energy norm, according to the smoothness of the resulting stress distribution in the continuum. The energy norm is generally calculated according to the following equations (Zienkiewicz & Craig 1986):

$$\|e_\sigma\|^2 = \int_v \{e_\sigma\}^T E^{-1} \{e_\sigma\}\, dv \tag{1}$$

where

$$e_\sigma = \sigma^* - \hat{\sigma} \tag{2}$$

and
σ^* is the element nodal stress
$\hat{\sigma}$ is the smooth average stress
E in Eqn (1) is the elasticity matrix and v is the domain of integration.

In a discretized form Eqn (1) can be written as

$$\|e_\sigma\|^2 = \sum_{i=1}^{m} \|e_\sigma\|_i^2 \tag{3}$$

where m is the number of elements used to discretize the continuum. The percentage error in the energy norm, h, is defined as

$$h = \left(\frac{\|e_\sigma\|^2}{\|U^*\|^2 + \|e_\sigma\|^2} \right)^{1/2} \times 100 \tag{4}$$

where U^* represents the calculated strain energy of the system. In this approach it is apparent that no exact solution needs to exist in order to assess the deviation of the finite element solution from the true response of the system. The criteria in Eqns (1–4) are usually acceptable from an engineering stand point, since for most problems there is no such exact solution unless many modifications and idealizations are introduced to the problem, in which case a so-called exact solution may be obtained using the basic equations of the theory of elasticity.

In this paper another more conventional approach has been pursued in order to assess the goodness of a given finite element mesh by simply comparing the results with existing exact solution according to the theory of elasticity. To this end, the following three examples were selected:

(a) Flexure of a cantilever prismatic member with a square cross-section.
(b) Flexure of a cantilever prismatic member with a circular cross-section.
(c) Twisting of a frustum shaft.

The three examples have a solution according to the theory of elasticity using the semi inverse method explained by Timoskenko & Goodier (1970). In the first two examples the dominant stress components are the axial and shear stress components $\sigma_x \tau_{xy}$, respectively. The main difference is the smooth cross-sectional boundaries in the circular cantilever opposite to the sharp corners that exist in the square cantilever. In the third example the solution, according to the theory of elasticity, reveals that there is no axial stress altogether. The variations in the spatial properties and the resulting stress field serve the intended study. The three cases have one factor in common which is that the dimension along the member axis is one order of magnitude higher than the cross-sectional dimensions.

The well known STRUDL finite element package was used to provide the finite element solution. Four (3-D) elements were used from STRUDL finite element library which are IPLS, IPLSCSH, IPLSCSH3 and TRIP. The first three elements are 8 node-elements while the last one is a 6-node element. A brief description of these elements is shown in Table 1 (Sperry Documentation Communiqué 1983).

In the following, the bastic equations of the theory of elasticity and the finite elements method are given with the intention of showing where the finite element approximation is introduced when solving the stress analysis boundary value problem. As indicated earlier, the reference solution was obtained using the theory of elasticity which is based on satisfying the following conditions expressed in indicial notation:

(a) Equilibrium equations

$$\sigma_{ij,\,j} + \rho b_i = 0 \tag{5}$$

where, in the absence of body couples, the stress tensor σ_{ij} is symmetric.

(b) Compatibility of strain equations

$$\varepsilon_{ij,\,km} + \varepsilon_{km,\,ij} - \varepsilon_{ik,\,jm} - \varepsilon_{jm,\,ik} = 0 \tag{6a}$$

Table 1. Three-dimensional STRUDL element used in the present study

Element name	Shape	No. of nodes	D.O.F.	Brief description
IPLS	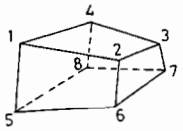	8	U_1, U_2, U_3	Linear displacement variation
IPLSCSH	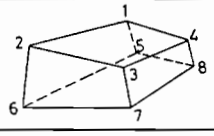	8	U_1, U_2, U_3	Linear displacement with constant shear
IPLSCSH3	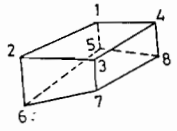	8	U_1, U_2, U_3	Linear displacement with constant shear distribution only in the global Z-direction
TRIP	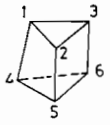	6	U_1, U_2, U_3	Linear displacement variation

where the Lagrangian linear strain-displacement equations are

$$\varepsilon_{ij} = \tfrac{1}{2}(u_{i,j} + u_{j,i}) \tag{6b}$$

Symmetry of the strain tensor is assumed in Eqns (6).

(c) Elastic constitutive equations

$$\sigma_{ij} = \frac{E}{1+\nu}\left(\varepsilon_{ij} + \frac{\nu}{1-2\nu}\,\delta_{ij}\varepsilon_{kk}\right) \tag{7}$$

(d) Boundary condition equations

$$n_i \sigma_{ij} = p_j \quad \text{on} \quad s_p \tag{8a}$$

where p_j represents the components of the surface traction per unit area and n_i is the unit outward normal to the surface.

$$u_i = u_i^p \quad \text{on} \quad s_u \tag{8b}$$

where

$$s = s_p + s_u \tag{8c}$$

and s represents the external surface of the continuum, s_p represents that portion of s where external traction p_j is specified, while s_u is the portion of s where displacements are prescribed.

The four tensorial Eqns (5–8) furnish a complete set for the solution of the boundary value problem of elastic stress analysis and the solution satisfying the four equations simultaneously is unique (Timoshenko & Goodier 1970).

Finding a closed form solution to the stress analysis boundary value problem is usually a complicated matter even for the simplest loading and boundary conditions. This led to the introduction of the semi-inverse approach commonly used in

texts on theory of elasticity (Timoshenko & Goodier 1970). This approach is based on assuming a stress field in terms of certain unknown parameters. These parameters are then determined in order to ensure the satisfaction of Eqns (5–8). In the close proximity of points of load application and support reactions, the solution according to the semi-inverse method may err but at distances sufficiently remote (equal to about the member depth) from load or reaction points the semi-inverse method should yield accurate results based on St. Venant principle. The reference exact solution, according to the theory of elasticity, for the three examples reported in this paper was obtained using the semi-inverse method.

In a displacement finite element formulation the continuum is discretized into elements and a suitable displacement function is then assumed for each element. The displacement function must satisfy certain conditions in order to ensure convergence of the solution in the limit as the element size tends to zero. Selecting a displacement function is basically the most important and cumbersome analytical step in the finite element analysis of a continuum. In certain cases, as in truss and beam members, there is, in principle, no need to assume a displacement function since the exact displacement function can be obtained by solving the governing field differential equations of equilibrium. Therefore the number of elements is totally irrelevant when modelling such members. This is not the case, however, when the exact displacement function can not be analytically obtained, as with the majority of 2-D and 3-D elements and a displacement function has to be assumed. In this latter case the mesh density and topology play a major role in determining the accuracy of the resulting solution.

Reverting to matrix notation, Eqns (6b) and (7) can be expressed as

$$\{\underline{\varepsilon}\} = [\underline{B}]\{\underline{u}\}. \tag{9}$$

Also

$$\{\underline{\sigma}\} = [E]\{\underline{\varepsilon}\} \tag{10}$$

where $\{\underline{u}\}$, $\{\underline{\varepsilon}\}$ and $\{\underline{\sigma}\}$ represent tensor fields for displacement, strains and stresses, respectively.

$[\underline{B}]$ is a matrix of differential operators and $[E]$ holds the elastic constants.

Applying the principle of virtual work is one way of completing the solution of the stress analysis boundary value problem. The principle states that "For a deformable body in equilibrium, the sum of virtual work done by the internal and external forces in arbitrary infinitesimal virtual displacements satisfying the prescribed geometrical boundary conditions is zero". Mathematically, this is expressed as

$$\int_v \{\delta\underline{\varepsilon}\}^T\{\underline{\sigma}\}\, dv - \int_{s_p} \{\delta\underline{u}\}^T\{\underline{p}\} s_p = 0 \tag{11}$$

where $\{\underline{\sigma}\}$ are the stresses resulting from external boundary traction $\{\underline{p}\}$, $\{\delta\underline{u}\}$ is a vector of admissible infinitesimal virtual displacements and $\{\delta\underline{\varepsilon}\}$ is the vector of generated virtual strains, "v" designates the domain of integration and s_p describes that portion of the boundary on which traction is prescribed. Substituting Eqns (9–10) in Eqn (11) and realizing that Eqns (9–10) are valid for both real or virtual displacements, we obtain

$$\int_v \{\delta\underline{u}\}^T[\underline{B}]^T[E][\underline{B}]\{\underline{u}\}\, dv - \int_{S_p} \{\delta\underline{u}\}^T\{\underline{p}\}\, dS_p = 0. \tag{12}$$

Eqn (12) may be viewed as a continuous force-deformation relationship in the presence of a continuous perturbation $\{\delta \underline{u}\}$.

The finite element approximation is introduced at this point where the continuous integration in Eqn (12) is replaced by summation over discrete elements. A continuous displacement function is assumed for each element such that the displacement at any point within the element domain $\{\underline{u}\}_e$ is uniquely defined in terms of the element nodal displacement $\{u\}$.

For a generic finite element let the assumed displacement function $\{\underline{u}\}_e$ be

$$\{\underline{u}\}_e = \{N\}\{u\}_e \tag{13}$$

where $\{N\}$ holds the shape functions and $\{u\}_e$ is the element generalized nodal displacements. The assumed displacement functions within each element $\{u\}_e$ must satisfy certain basic requirements as indicated, for example, by Martin & Carey (1973). Elements meeting those conditions are referred to as conforming elements. Other non-conforming elements may still be used and give satisfactory results. Modelling errors may arise if any of the conformity conditions has been violated regardless of the fineness of the finite element mesh. This is mathematically referred to as divergence of a finite element solution. If, however, the displacement function is correctly chosen, the number and orientation of the elements play a significant role in determining the degree of solution accuracy. Errors arising in this case are referred to as discretization errors and can be estimated using the energy norm "h" defined in Eqn (4) or other similar criteria.

Substituting Eqn (13) into Eqn (12) and cancelling out the virtual displacements $\{\delta \underline{u}\}$, and realizing that

$$\{\delta \underline{u}\}_e = \{N\}\{\delta u\}_e \tag{14}$$

we get

$$\sum \int_{v_e} [B]^T[E][B]\, dv_e \{u\}_e = \sum \{p\} \tag{15}$$

where

$$[B] = [\underline{B}]\{N\} \tag{16}$$

and

$$\{p\} = \int_{S_{pe}} \{N\}^T\{p\}\, ds_{p_e}. \tag{17}$$

If some of the traction forces are acting at the nodes as concentrated loads, their contribution should be added separately to the R.H.S in Eqn (15).

Eqn (15) can then be re-cast as

$$\sum [k]_e\{u\}_e = \sum \{p\} \tag{18}$$

where

$$[k]_e = \int_{v_e} [B]^T[E][B]\, dv_e.$$

The summation in Eqn (18) is to be performed vectorially over the active elements using any suitable assembling technique to yield the general structural force

deformation relationships

$$[K]\{U\} = \{P\} \tag{19}$$

where

$$[K] = \sum [k]_e \tag{20}$$

and

$$\{P\} = \sum \{p\}. \tag{21}$$

Prescribed displacements u_i^p on S_u in Eqn (8b) can be easily incorporated into Eqn (18) using matrix partitioning techniques (Prezemieniecki 1968).

It may be noted that the basic equations of the theory of elasticity, Eqns (5–8), have all been used in the derivation of the finite element formulations except Eqns (5) and (6a) which are the equilibrium and compatibility equations respectively. The equilibrium equations are already incorporated into Eqn (12) since the principle of virtual work assumes equilibrium of the stressed body. The satisfaction of the compatibility of strains, hence stresses, as implied by Eqn (6a) has not been invoked into the finite element formulation. Compatibility of strains and stresses are mainly dependent on the type of displacement function selected for the element. Within each element the strains are continuous but across element interfaces this may not necessarily be so. The smoothness of the resulting distribution may be taken as one measure of the errors involved due to the discretization process as shown in Eqns (1–4). Finite element displacement formulation will guarantee equilibrium at the nodes but not along the interfacing edges. Displacements, however, will be continuous throughout the continuum when conforming elements are used. Hybrid formulation, on the other hand, ensures equilibrium everywhere but displacement compatibility ensures equilibrium only at the nodes. Mixed formulation combines some of the features of both formulations.

The question of bounds on the finite element solution is important and useful in some cases. Only when conforming elements are used does a mathematical proof exist which furnishes bounds on the resulting solution. It is known from the principle of minimum potential energy that the exact displacements corresponding to equilibrium are those which will bring the structural total potential energy to a minimum, i.e.

$$\delta\pi_p = 0 \tag{22}$$

where

$$\pi_p = W + U^*. \tag{23}$$

W is the external work done and U^* is the induced strain energy. Therefore any non-exact displacement pattern will always overestimate the structural total potential energy π_p. It may be then concluded that any approximate solution, including a finite element solution, will always be an upper bound to the true structural potential energy π_p. It may be also proved, using the energy conservation principle, that any approximate solution will simultaneously furnish a lower bound to the structural strain energy U^* (Zienkiewicz 1971). Unfortunately the bounds discussed above are of limited usefulness since, in general, neither deflections nor stresses can be bounded.

This paper intends to discuss the effect of certain discretization and modelling parameters on the accuracy of stress prediction in the context of 3-D linear elastic analysis. Three examples were selected for which a so-called exact solution for stresses exists according to the theory of elasticity. Each of the three examples is presented in the following, whereas the discussion pertaining to each application is presented at the end of each case.

CASE I—BENDING OF A SQUARE CANTILEVER

Figure 1 shows a cantilever having a square cross-section subjected to a concentrated load at its tip. When the semi-inverse method is applied, the resulting non-zero stress components are (Timoshenko & Goodier 1970)

$$\sigma_x = -\frac{P(L-x)y}{I_z} \tag{24}$$

$$\tau_{yx} = \frac{P}{2I_z}(a^2 - y^2) + \frac{\partial \phi}{\partial z} \tag{25}$$

$$\tau_{zx} = -\frac{\partial \phi}{\partial y}.$$

The stress function ϕ takes the form

$$\phi = A \sum_{m=0}^{m=\infty} \sum_{n=1}^{n=\infty} R_{2m+1,n} \cos \frac{(2m+1)\pi y}{2a} \sin \frac{n\pi z}{a} \tag{26}$$

where a is equal to half side length of the cross-section.

Differentiating Eqn (26) with respect to y and z, the shearing stresses τ_{yx} and τ_{zx} can be expressed as

$$\tau_{yx} = \frac{P}{2I_z}(a^2 - y^2) + A \sum_{m=0}^{m=\infty} \sum_{n=1}^{n=\infty} R_{2m+1,n} D_n \cos C_m y \cos D_n z \tag{27}$$

$$\tau_{zx} = A \sum_{m=0}^{m=\infty} \sum_{n=1}^{n=\infty} R_{2m+1,n} C_m \sin C_m y \sin D_n z \tag{28}$$

where

$$A = \frac{-8a^3 vp}{(1+v)I_z \pi^4} \tag{29}$$

$$R_{2m+1,n} = \frac{(-1)^{m+n-1}}{(2m+1)n[((2m+1)^2/4) + n^2]} \tag{30}$$

$$C_m = \frac{(2m+1)\pi}{2a} \tag{31}$$

$$D_n = \frac{n\pi}{a}. \tag{32}$$

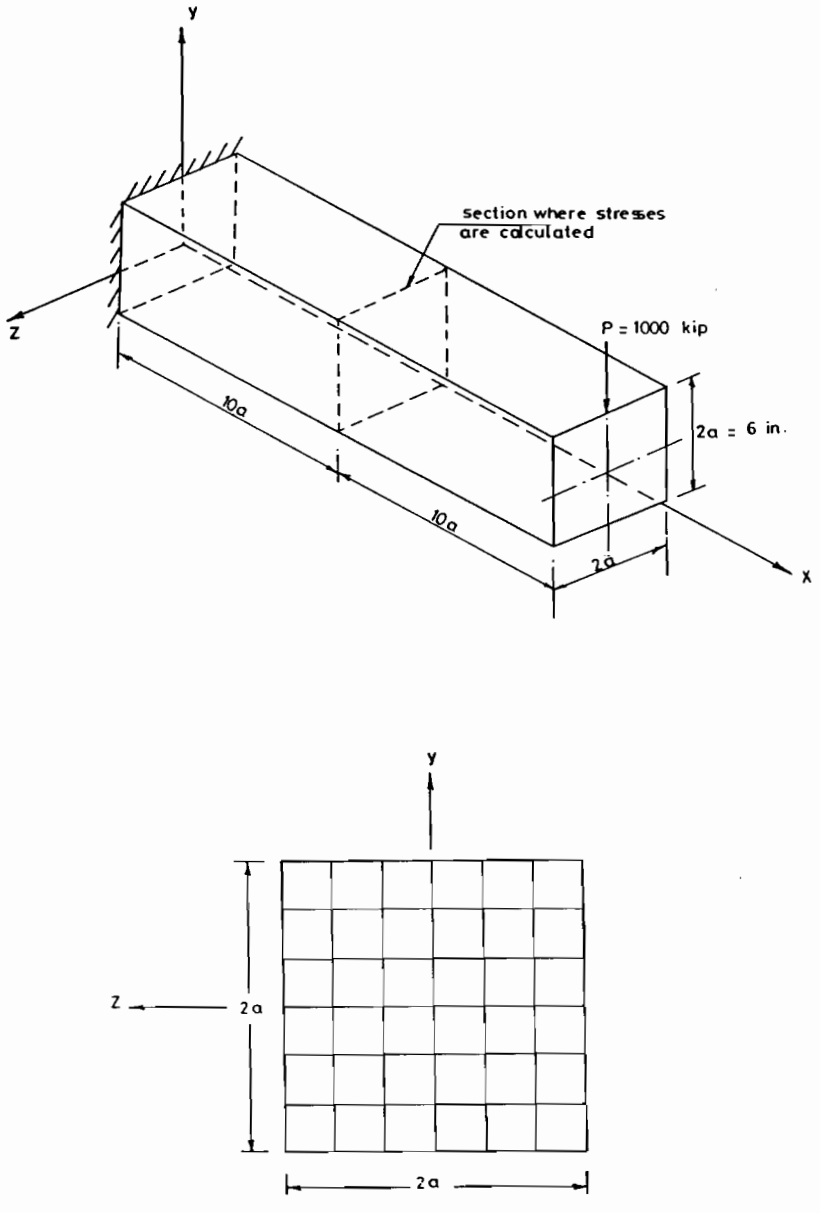

Fig. 1. Bending of a prismatic square cantilever—Cross-section divisions shown (1 inch = 25·4 mm, 1 Kip = 4·45 kN).

Equations (24–32) completely describe the stress state in the continuum. However, a sufficiently large number of terms must be retained in the summations shown in Eqns (26–28) in order to ensure accuracy. The finite element solution by STRUDL was obtained for the four elements shown in Table 1, namely IPLS, IPLSCSH, IPLSCSH3 and TRIP elements. Stresses calculated according to STRUDL are the average nodal stresses for all the elements meeting at a particular node.

Stresses predicted according to the two methods were calculated at a cross-section located half-way along member length (Fig. 1), in order to minimize the stress concentration effects at the loading and supporting points.

a. Effect of element type

A uniform mesh involving 1440 elements and 2009 nodes was used. Fig. 1 shows that 6 divisions per side of the cross-section were used. In the longitudinal direction, along the member axis, 40 divisions were considered. Fig. 2 shows a 3-D view of part of the discretized member and the element side ratio. This grid was used for IPLS, IPLSCSH, IPLSCSH3 elements. For the TRIP element the finite element grid in Fig. 3 was used which involved 2009 nodes but eventually double the number of elements (2880). The effect of element type on each stress component is now presented.

Before discussing the accuracy of the finite element soluion by STRUDL, it may be indicated that the percentage relative error as shown in Tables 2–7 was calculated according to the following relationship:

$$\text{Relative error} = \frac{\sigma^* - \sigma}{|\sigma^*|} \times 100 \tag{33}$$

where σ^* is the largest stress value predicted by the theory of elasticity along a prescribed section, and σ is the corresponding value predicted by STRUDL.

From Table 2, all the elements predict σ_x with sufficient accuracy, where the table gives the relative error for each element as calculated for the stress at the outermost fiber of the cross-section. Elements IPLS and IPLSCSH, however, give

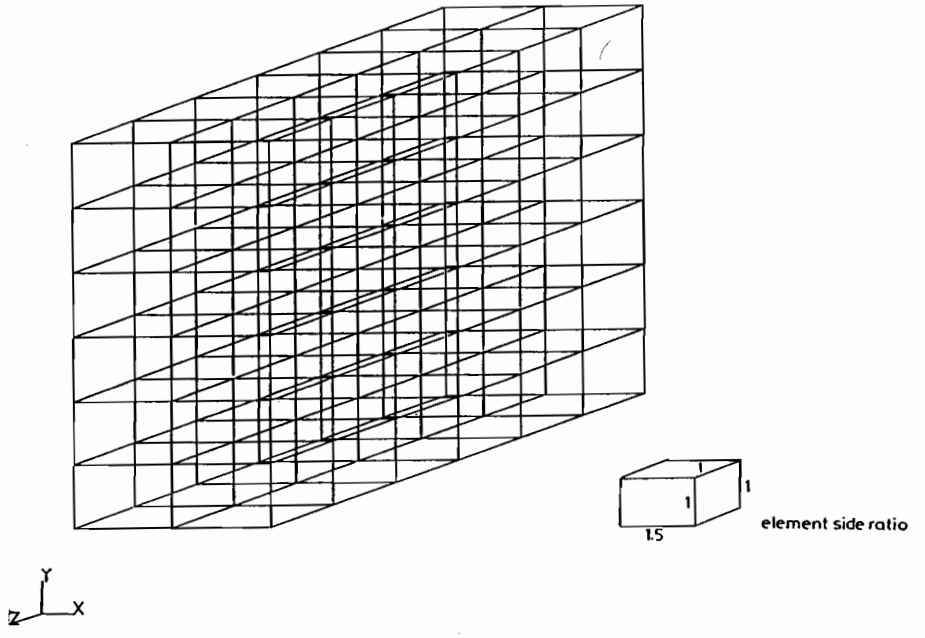

Fig. 2. Finite element grid for STRUDL using 1440 8-node element (only part of the member is shown).

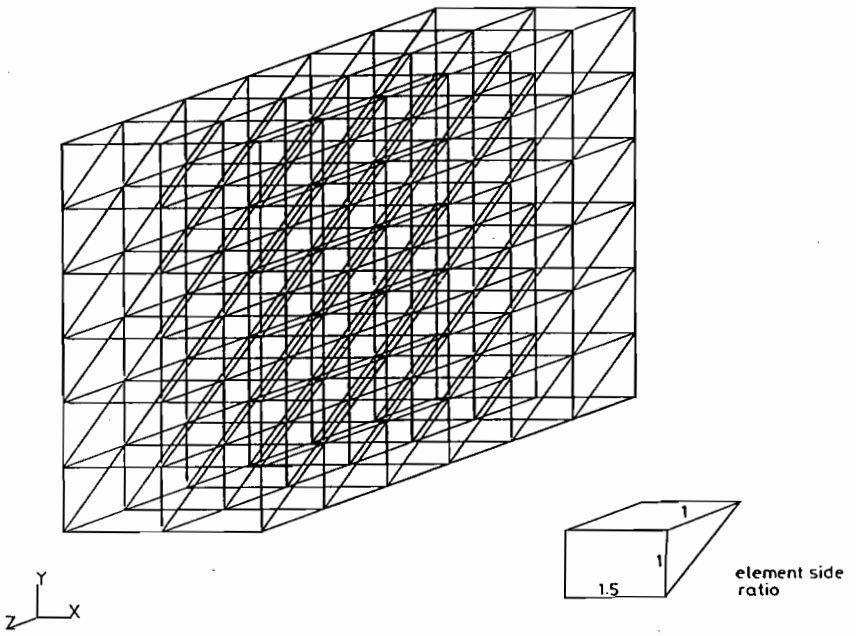

Fig. 3. Finite element grid for STRUDL using 2880 6-node elements (only part of the member is shown).

the highest accuracy. The nodal stress prediction for all elements show a linear distribution for σ_x across the member depth (Fig. 4a). It may be indicated that when plotting the stress distribution the stresses were assumed to change linearly within each element.

Figure 4b shows the distribution of τ_{xy} along the section ($z = 0$) using IPLS element. The finite element solution underestimated τ_{xy} at the center (maximum value) but consistently gives a value different from zero at the member faces ($y = \pm a$). This behaviour is typical for all elements used. Table 2 shows that element IPLSCSH3 gives the best accuracy (4·95%). Along a horizontal section ($y = 0$), the prediction of the two methods is shown in Fig. 4c. All elements provide good prediction for both the magnitude and the general shape of the distribution.

The distribution of τ_{xz} along section ($z = -2a/3$) is shown in Fig. 4d for the IPLS element along with the theory of elasticity solution. Table 2 indicates that all

Table 2. Relative errors for the example of bending of a square cantilever using 1440 elements

Stress component	Type of element			
	IPLS	IPLSCSH	IPLSCSH3	TRIP
σ_x	0·0126%	0·0399%	−2·3550%	1·0450%
τ_{xy}	9·56%	9·70%	4·96%	8·89%
τ_{xz}	18·70%	11·46%	16·80%	15·95%

Notes:

1. Maximum stress values along line $z = 0$ were used for σ_x and τ_{xy}.
2. Maximum stress values along $z = 2a/3$ were used for τ_{xz}.

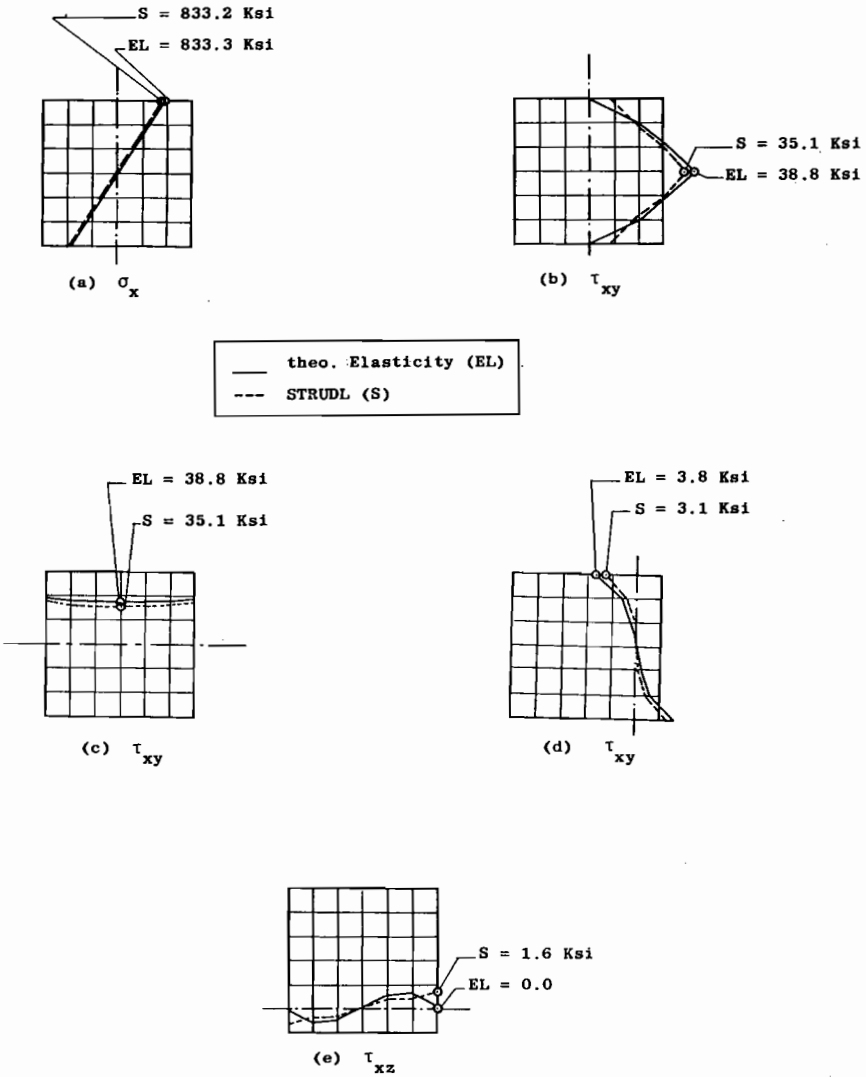

Fig. 4. Stress distribution using theory of elasticity and STRUDL (1440 IPLS elements) (1 Ksi = 6.89 MPa).

elements give high relative error; however elements IPLSCSH give the least error of 11·46%. For the section along ($y = -2a/3$) the situation is different; according to the theory of elasticity τ_{xz} along the edges $z = \pm a$ must be identically zero according to Eqns (28) and (32), since (sin $n\pi$) is always zero for any integer values of n. Fig. 4e shows the distribution of τ_{xz} using IPLS element along the section at $y = -2a/3$, where the error is maximum along the edges. All elements give values different from zero along the edges $z = \pm a$. The maximum error in edge stress prediction was given by TRIP element and is shown in Fig. 5. Notice that τ_{xz} is, in general, small compared to the other stress components τ_{xy} and σ_x under the given loading and support conditions.

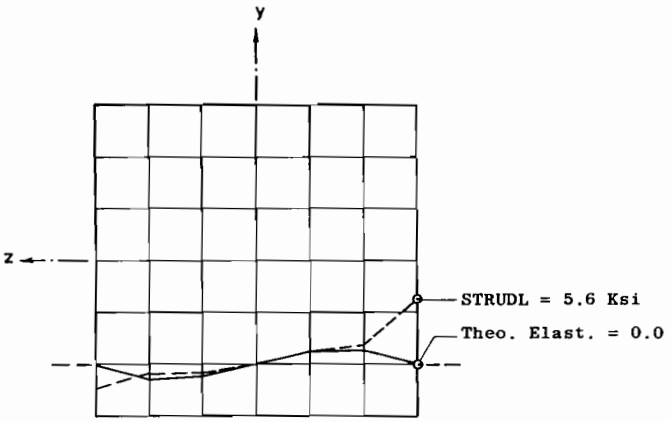

Fig. 5. τ_{xz} Distribution using theory of elasticity and STRUDL (2880 TRIP elements) (1 Ksi = 6·89 MPa).

b. Effect of element side ratio

The object of this part of the study is to evaluate the effect of distorting element dimensions on the resulting solution accuracy. Element IPLSCSH has been exclusively used in this part of the study. The cross-section divisions were kept unaltered at six divisions per side, whereas the longitudinal divisions along the x axis were allowed to vary. Three element side ratios were used as indicated in the inset of Figs 2, 6 and 7. Table 3 summarizes the results of the three grids.

c. Discussion

1. Table 2 indicates that σ_x can be accurately predicted using 1440 elements at the element side ratio 1 : 1 : 1·5 shown in Fig. 2, using either IPLS or IPLSCSH elements. The error when using IPLSCSH3 or TRIP elements is higher by two orders of magnitude. The error involved in calculating τ_{xy} is significantly high but has the same order of magnitude for all elements. The situation is compounded for τ_{xz} where errors of more than 18% are obtained.

Fig. 6. Finite element grid for STRUDL using 720 8-node elements.

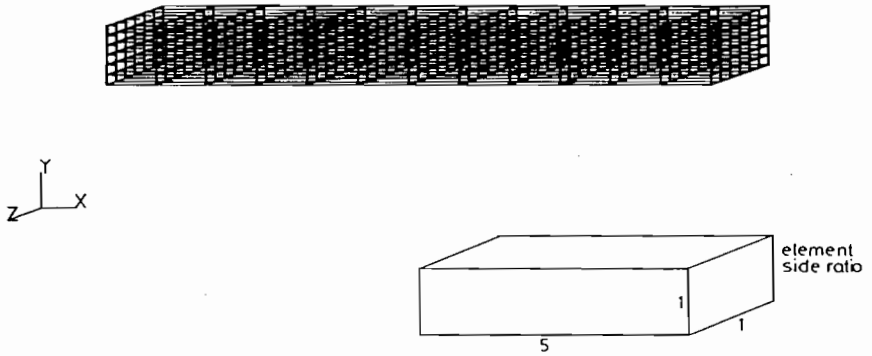

Fig. 7. Finite element grid for STRUDL using 432 8-node elements.

2. From Fig. 4 it may be noted that the finite element solution consistently experiences certain difficulties along the edges if the stress component is supposed to vanish. The theoretical zero τ_{xy} values along edges $y = \pm a$ could not be predicted by any of the elements as well as the zero τ_{xz} values along edges $z = \pm a$. It has been shown (Connor & Will 1979) that the element stress nodal average often yields good results for stress calculations at the interior points. Along the edges, however, the element nodal average is not usually a satisfactory method for calculating the stresses, which may explain the large discrepancy of shear stress prediction along the edges.
3. The effect of distorting element dimensions in the axial direction is clearly reflected in Table 3. The accuracy in calculating the stress components deteriorates rapidly indicating the significance of the element side ratio on solution accuracy. The relatively fine mesh of 1440 elements may be accurate enough for σ_x but it is not so for the shear components τ_{xy} and τ_{xz}.

CASE II—BENDING OF A CIRCULAR CANTILEVER

Figure 8 shows a cantilever beam of a circular cross-section loaded in bending and shear by a concentrated load at the free end. Applying St. Venant semi-inverse

Table 3. Relative errors for the example of bending of a square cantilever using IPLSCSH elements

	Stress components		
No. of elements	σ_x	τ_{xy}	τ_{xz}
1440 Fig. 2	0·0400%	9·70%	11·46%
720 Fig. 6	6·59%	25%	17%
432 Fig. 7	41·60%	54·65%	42·55%

Notes:
1. Maximum stress values along line $z = 0$ were used for σ_x and τ_{xy}.
2. Maximum stress values along line $z = -2a/3$ were used for τ_{xz}.

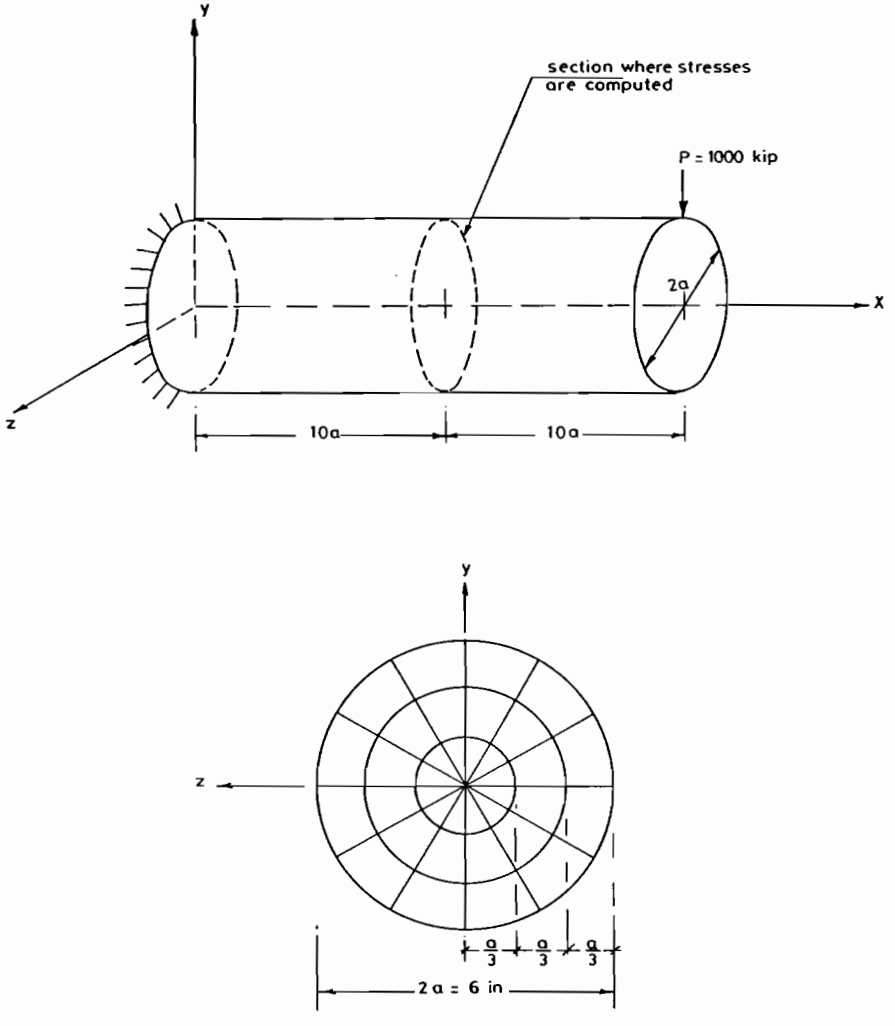

Fig. 8. Bending of a prismatic circular cantilever—Cross-section divisions shown (1 inch = 25·4 mm, 1 Kip = 4·45 kN).

method, the non-zero stress components are (Timoshenko & Goodier 1970)

$$\sigma_x = \frac{-P(L-x)y}{I_z} \tag{34}$$

$$\tau_{yx} = \frac{-(1+2v)P}{4(1+v)I_z}\left(r^2 - y^2 - \frac{1-2v}{3+2v}z^2\right) \tag{35}$$

$$\tau_{zx} = \frac{-(1+2v)Pyz}{4(1+v)I_z} \tag{36}$$

Fig, 8 also shows the cross-sectional divisions used throughout this example which involves 36 divisions.

a. Effect of element type

Only three 8-node elements were considered in this comparison. The 6-node TRIP element was used with each of the three 8-node elements IPLS, IPLSCSH, IPLSCSH3 in order to model the first layer of elements with a common vertex along the member's axis. A finite element mesh involving 1440 elements was used in this study where 40 divisions were used along the member axis. Fig. 9 shows the finite element grid, for only part of the member, along with the elements side ratio. The curved boundaries were always approximated by straight lines as shown in Fig. 9.

Figure 10 shows the distribution of σ_x, τ_{xy} and τ_{xz} when elements IPLSCSH and TRIP were used for modelling the cantilever. Notice that σ_x and τ_{xy} distribution is plotted along the y axis while τ_{xz} is plotted on an axis at 30° to the y axis since τ_{xz} assumes the highest values along this diameter as compared to the rest of the radial lines shown in Fig. 8.

Table 4 summarizes the results of the comparison where the three elements give comparable results. Element IPLSCSH3, however, gives better prediction for τ_{xy} and τ_{xz} but larger errors are involved in its prediction for σ_x. It may be also noted that σ_x is overestimated by the three elements while τ_{xy} and τ_{xz} are underestimated.

b. Effect of element side ratio

In this part of the investigation the cross-sectional divisions in the z-y plane, which included 3 circles and 12 radial lines, were kept unaltered while the number of longitudinal divisions along the x-axis was allowed to vary. Three cases were considered as shown in Figs 9, 11 and 12, where the elements dimension in the x direction

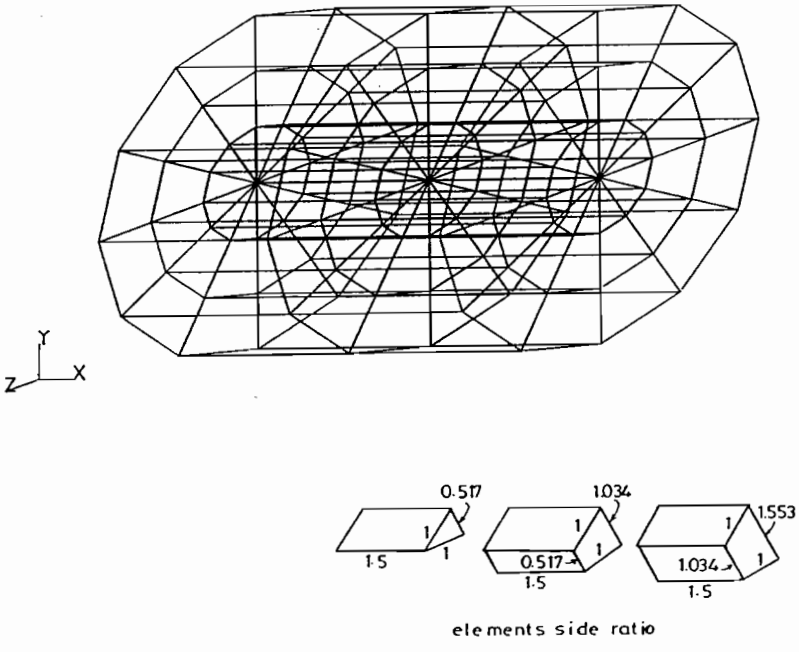

Fig. 9. Finite element grid for STRUDL using 1440 elements (only part of the member is shown).

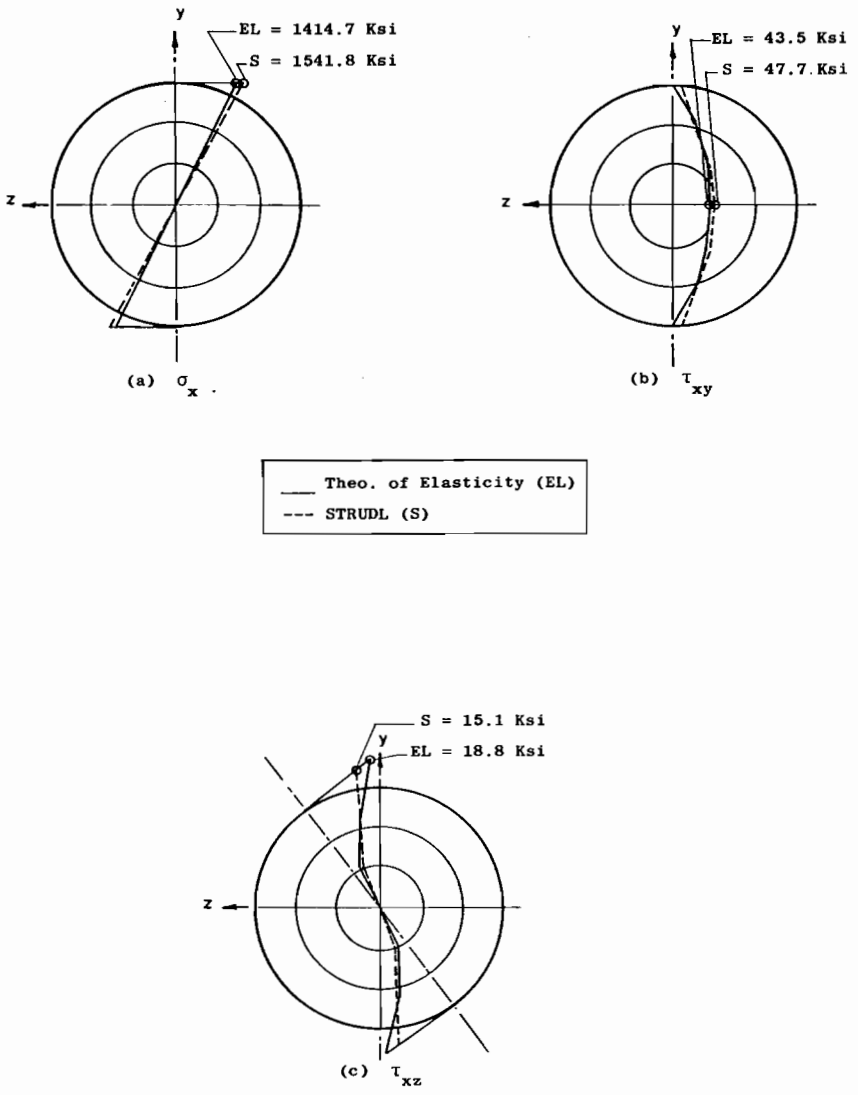

Fig. 10. Stress distribution using theory of eleasticity and STRUDL (1440 IPLSCSH and TRIP elements) (1 Ksi = 6·89 MPa).

increases progressively resulting in small number of elements. In Fig. 11, 720 elements were used while in Fig. 12, 432 elements were employed.

Table 5 shows the relative error as obtained in each case. It may be noted that even the relatively fine mesh of 1440 elements errs by more than 20% for the τ_{xz} stress component. The error with the 432 element grid is more than 63% for τ_{xy} as shown in Fig. 13.

c. Discussion

1. For the particular application of the circular cantilever beam, it may be concluded that the IPLSCSH element, together with TRIP element for the inner

Table 4. Relative errors for the example of bending of a circular cantilever using 1440 elements

Stress component	Type of element		
	IPLS & TRIP	IPLSCSH & TRIP	IPLSCSH3 & TRIP
σ_x	−9·02%	−8·99%	−12·20%
τ_{xy}	3·690%	2·649%	0·004%
τ_{xz}	23·70%	20·15%	18·48%

Notes:

1. Maximum stress values along z axis were used for σ_x and τ_{xy}.
2. Maximum stress values along an inclined axis (Fig. 10c) were used for τ_{xz}.

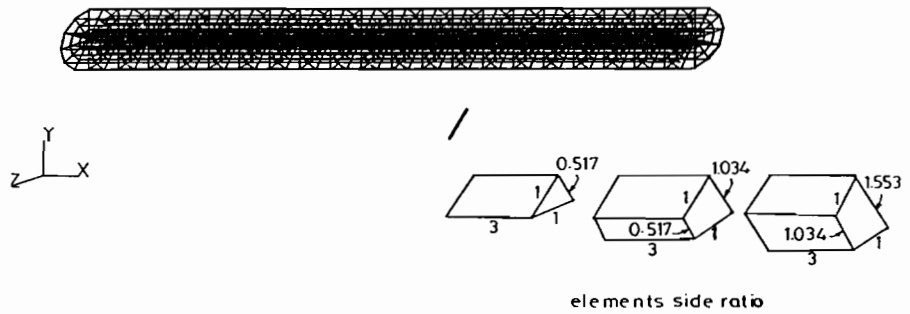

Fig. 11. Finite element grid for STRUDL using 720 elements.

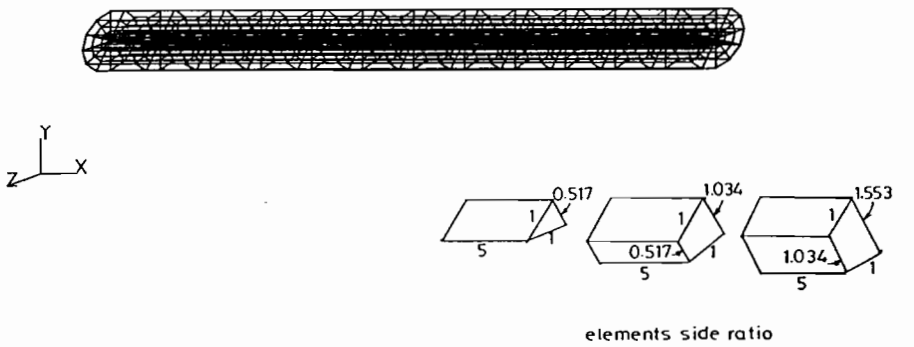

Fig. 12. Finite element grid for STRUDL using 432 elements.

layer, give the best overall average accuracy. The relative, error in predicting $(\sigma_x)_{max}$ is about 8·9% while in predicting $(\tau_{xy})_{max}$ it is about 2·6%. As for $(\tau_{xz})_{max}$ the error increases to about 20%.

2. The effect of element side ratio is clear in this application where the accuracy deteriorates rather rapidly for the coarser grids. From Table 5 it may be noted that the stress component τ_{xz} was not too sensitive to element distortion in the axial direction as compared to the other stress components σ_x and τ_{xy}.

Table 5. Relative errors for the example of bending of a circular cantilever using IPLSCSH and TRIP elements

No. of elements	Stress component		
	σ_x	τ_{xy}	τ_{xz}
1440 Fig. 9	−8·99%	2·65%	20·15%
720 Fig. 11	0·60%	24·55%	27·18%
432 Fig. 12	17·64%	63·70%	38·10%

Notes:
1. Maximum stress values along z axis were used for σ_x and τ_{xy}.
2. Maximum stress values along an inclined axis (Fig. 10c) were used for τ_{xz}.

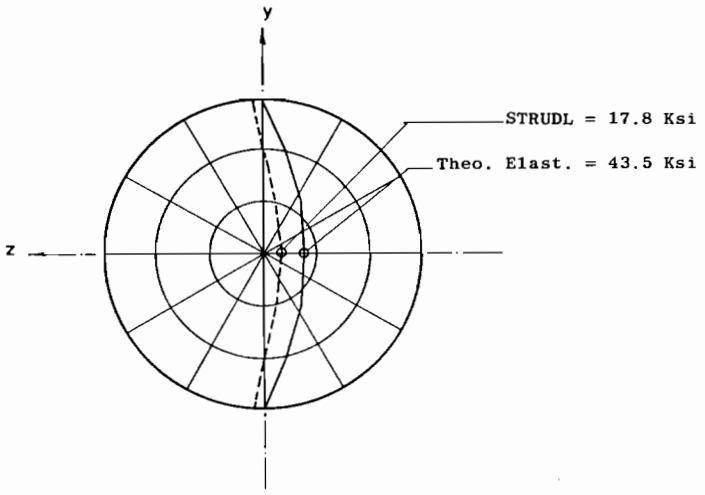

Fig. 13. τ_{xy} Distribution using theory of elasticity and STRUDL (432 IPLSCSH and TRIP elements) (1 Ksi = 6·89 MPa).

CASE III—TORSION OF A SHAFT WITH VARIABLE CROSS-SECTION

Figure 14 shows a frustum shaft subjected to torsion at the narrow end while the other wide end is fixed. The semi-inverse method is also applied in this case where it is assumed that the axial and radial displacements are identically zero while the tangential displacement is different from zero.

According to the previous assumptions the non-zero stress components for the frustum shaft in terms of the cylinderical coordinates (x, r, θ) are (Timoshenko & Goodier 1970)

$$\tau_{\theta x} = \frac{-Cr(L-x)}{(r^2-x^2)^{5/2}} \tag{37}$$

$$\tau_{r\theta} = \frac{-Cr^2}{(r^2+x^2)^{5/2}} \tag{38}$$

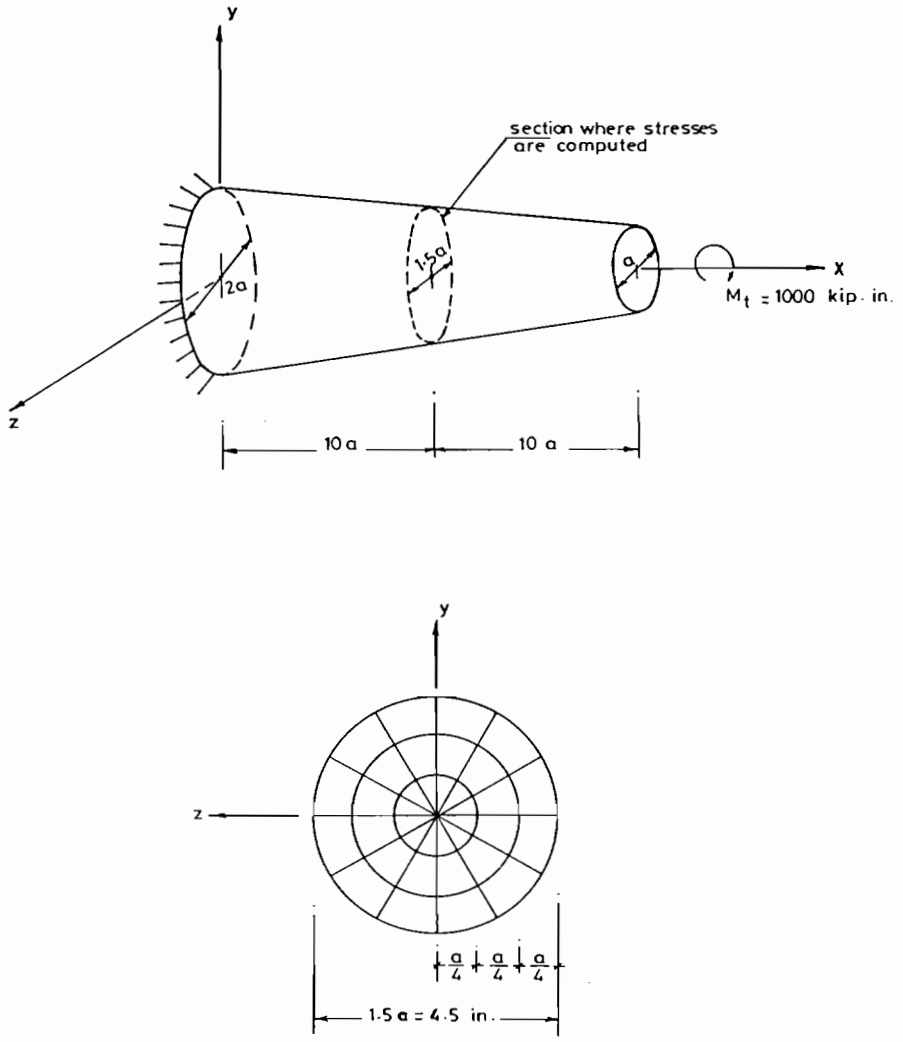

Fig. 14. Twisting of a frustum shaft—Cross-section divisions shown (1 inch = 25·4 mm, 1 Kip = 112·98 kN mm).

where

$$C = \frac{-M_t}{2\pi(\frac{2}{3} - \cos\alpha + \frac{1}{3}\cos^3\alpha)} \tag{39}$$

and

$$\alpha = \cos^{-1}\frac{L - x}{[r^2 + (L - x)^2]^{1/2}} \tag{40}$$

is the semi-vertex angle of the shaft. L is the length of the frustum shaft. It may be mentioned here that it is always better to calculate the constant C in Eqn (39) using

double precision since its value was found to be sensitive to round-off errors particularly for small semi-vertex angle α. It is noted that the stresses given in Eqns (37 and 38) are the cylindrical components whereas STRUDL prediction is given in terms of the cartesian components.

The relationship between the two stress tensors is thus defined by the orthogonal transformation relationship

$$\sigma'_{ij} = \beta_{ip}\beta_{jq}\sigma_{pq} \tag{41}$$

where σij is the cartesian stress tensor, and $\sigma' ij$ is the cylindrical stress tensor, βij is an orthogonal transformation tensor given by

$$(\beta_{ij}) = \begin{vmatrix} 1 & 0 & 0 \\ 0 & \cos\theta & -\sin\theta \\ 0 & \sin\theta & \cos\theta \end{vmatrix}, \tag{42}$$

and

$$\theta = \tan^{-1}\frac{y}{z}. \tag{43}$$

The cross-sectional divisions are shown in Fig. 14 involving three circles and twelve radial lines.

a. Effect of element type

For this study three 8-node elements were tried, namely IPLS, IPLSCSH and IPLSCSH3. The TRIP 6-node element was used with each of the 8-node elements in order to model the first layer of elements with a common vertex along the shaft axis. A total of 40 divisions were used along the shaft axis. The finite element mesh for only part of the shaft is shown in Fig. 15 along with element side ratio for both of the narrow and wide faces of the frustum shaft. Fig. 16 shows the distribution of τ_{xz} and τ_{xy} according to the theory of elasticity and STRUDL using IPLS element. Table 6 shows the relative errors involved in the prediction of STRUDL using each of the three elements. τ_{xz} assumed the highest values along the y axis as indicated in Fig. 16a but the largest value for τ_{xy} occurs along the radial line making 60° with the y axis (Fig. 16b), which was used in the comparison.

b. Effect of element side ratio

Two other finite element grids were tried in order to study the effect of element distorsion in the axial direction on the solution accuracy; the grids are shown in Figs 17 and 18. Table 7 shows the results of the comparison for the three tested grids.

c. Discussion

1. For the application of a frustum shaft under end torque it is concluded that the combination of IPLS element with TRIP element gives the most accurate results as compared to the other tested 8-node elements. All elements successfully predicted the general shape of the distribution with varying accuracy.

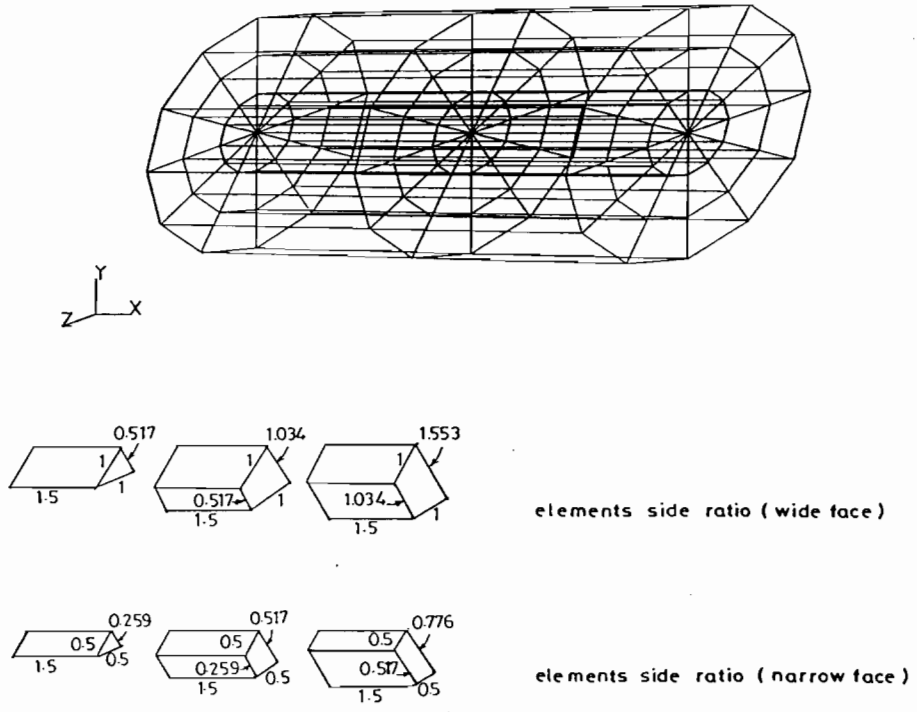

Fig. 15. Finite element grid for STRUDL using 1440 elements (only part of the member is shown).

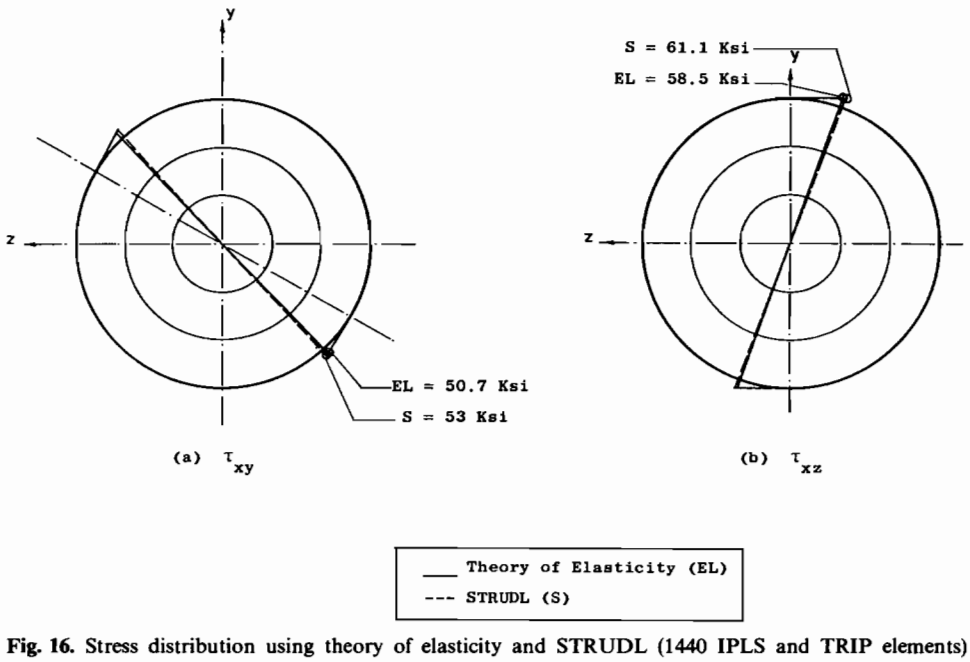

Fig. 16. Stress distribution using theory of elasticity and STRUDL (1440 IPLS and TRIP elements) (1 Ksi = 6·89 MPa).

Table 6. Relative errors for the example of twisting a frustum shaft using 1440 elements

Stress component	Type of element		
	IPLS	IPLSCSH	IPLSCSH3
τ_{xy}	−4·54%	−5·87%	−12·66%
τ_{xz}	−4·53%	−10·32%	−12·54%

Notes:
1. Maximum stress values along y axis were used for τ_{xy}.
2. Maximum stress values along an inclined axis (Fig. 16a) were used for τ_{xz}.

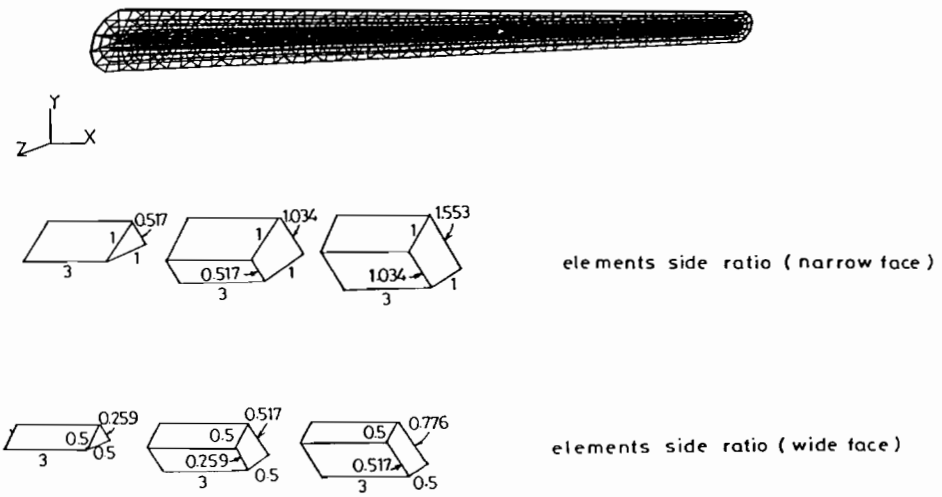

Fig. 17. Finite element grid for STRUDL using 720 elements.

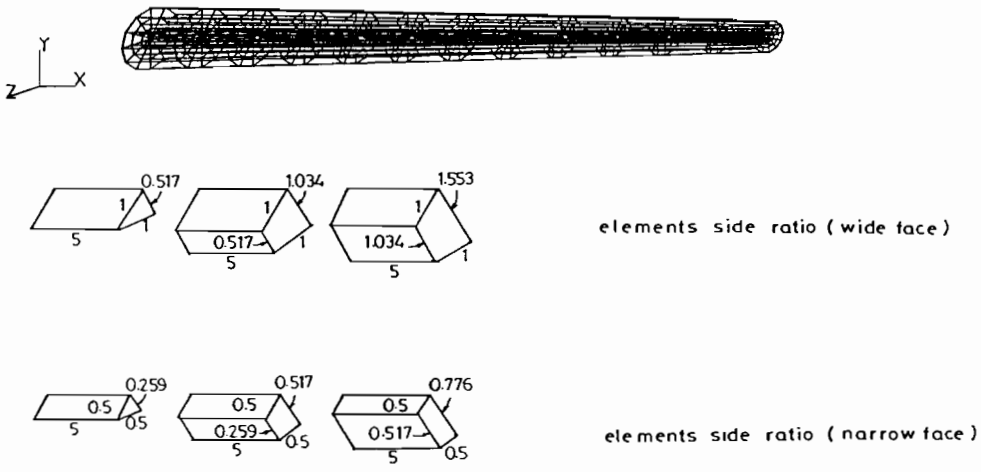

Fig. 18. Finite element grid for STRUDL using 432 elements.

2. The effect of increasing the element dimension in the axial direction is clearly less significant in the present example than in the previous two examples. From Table 7 it may be noted that even with the severely distorted elements shown in Fig. 18, STRUDL solution gives a relative error of about 2% for τ_{xy} and τ_{xz}. Fig. 19 shows the distribution of the two stress components using a coarse mesh (Fig. 18), involving 432 elements.

Table 7. Relative errors for the example of twisting a frustum shaft using 720 IPLS and TRIP elements

No. of elements	Stress component	
	τ_{xy}	τ_{xz}
1440 Fig. 15	−4·54%	−4·53%
720 Fig. 17	−4·69%	−4·62%
432 Fig. 18	2·174%	2·197%

Notes:
1. Maximum stress values along y axis were used for τ_{xy}.
2. Maximum stress values along an inclined axis (Fig. 16a) were used for τ_{xz}.

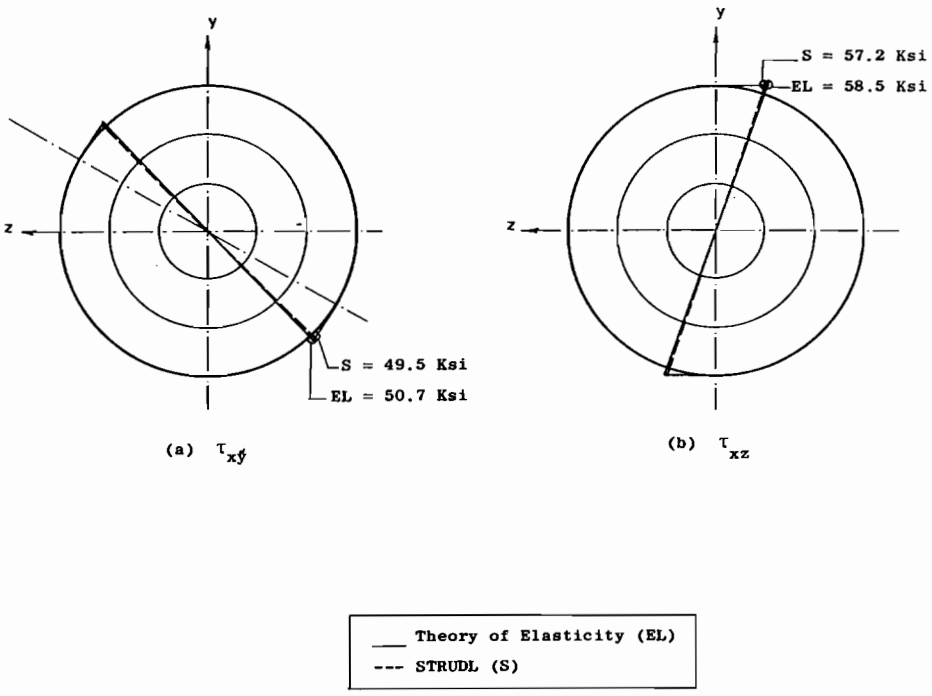

Fig. 19. Stress distribution using theory of elasticity and STRUDL (432 IPLS and TRIP elements (1 Ksi = 6·89 MPa).

CONCLUSIONS

1. The subject of errors and accuracy of a finite element solution is important and the issue is presently attracting several researchers in the field. A recent publication (Naief & Al-Hussaini 1990) addressed the errors involved in 2-D finite element analysis as compared to the exact theory of elasticity solution and the practical strength of material approximate method. Structural and mechanical components such as beams and bars where the cross-sectional dimensions are of the same order of magnitude which is small compared with the axial dimension, often cause modelling problems when a 3-D finite element mesh is used. Selected mesh may tend to distort the elements in the longitudinal axial direction in order to end up with a reasonable number of elements. It has been demonstrated in this study that if both displacements and stresses are anticipated to be small in the axial direction, then the effect of element distortion in the axial direction may be tolerated as in the application of the frustum shaft in torsion. In the other two applications where axial stresses are dominant, the effect of axial distortion is significant. Tables 3, 5 and 7 clearly reflect this fact.
2. Element side ratio and the total number of elements used to descritize a long bar are actually interrelated. Clearly, finite element software users tend to distort the element axial dimensions in order to reduce the total number of elements involved in the discretization of long members. The problem is even compounded when it is necessary to put a 3-D finite element mesh on a thin-walled long member, such as steel rolled sections. In this latter case the three basic member spatial dimensions (length, overall section height and plates thickness) are all of different order of magnitude. If element distortion is to be avoided, a very large number of 3-D elements should be used for the discretization of thin-walled members.
3. No single element proved to give consistently better accuracy than the other elements for all stress components for all applications. However, for 3-D bending of bars, element IPLSCSH seems to give more consistent results than the other elements as noted from Tables 2 and 4. For twisting of bars the IPLS element tends to give better accuracy.
4. Tables 2–7 show that the finite element solution does not establish a specific upper or lower bound on stress values as the solution in some cases overestimates the stress value, while in other cases the finite element solution underestimates it. This is in agreement in substance, with the fact that finite element bounds are only valid for the potential and strain energies but not on stresses or deformations.
5. It has been quantitatively demonstrated that it is rather important to test element and mesh accuracy before applying them in real analysis and design situations. Unacceptably large errors may result if severely distorted elements are used. Accuracy can be also enhanced if some effort is spent in selecting the proper element to be used from the element library of the available software.
6. The discussion and the conclusions drawn at the end of each example are obviously limited to the particular application studied. The paper, however, may give an idea about the order of magnitude of the errors involved in similar applications.

ACKNOWLEDGEMENT

The authors would like to thank the Kuwait Foundation for the Advancement of Sciences for sponsoring this project (Grant No. 86-02-03).

REFERENCES

Babuska, I., Zeinkiewicz, O.C., Cago, J. & Oliveira, E.R. (Eds). 1986. Accuracy estimates and adaptive refinements in finite element computations. John Wiley & Sons, New York, 311 pp.

Connor, J. & Will, G. 1979. Computer-aided teaching of the finite element displacement method. M.I.T. Department of Civil Engineering Research Report R69-23. ICES Users Group Inc., 420 pp.

Martin, C.H. & Carey, G.F. 1973. Introduction to finite element analysis. McGraw-Hill, New York, 222 pp.

Naief, G. & Al-Hussaini, M. 1990. A comparison of strength of materials, elasticity and finite element method in 2-D problems. Journal of the University of Kuwait (Science) 17(1): 43–73.

Prezemieniecki, J.S. 1968. Theory of matrix structural analysis. McGraw-Hill, New York, 382 pp.

Sperry Documentation Communiqué. 1983. 1100 ICES STRUDL user guide. Application Development Center—Blue Bell. Document Number UA-0594, 1202 pp.

Timoshenko, S. & Goodier, J.N. 1970. Theory of elasticity. McGraw-Hill, New York, 567 pp.

Zienkiewicz, O.C. 1971. The finite element method in engineering science. McGraw-Hill, New York, 787 pp.

Zienkiewicz, O.C. & Craig, A. 1986. Adaptive refinements, error estimates, multigrid solution and hierarchic finite element concepts. In: **Babuska, I., Zienkiewicz, O.C., Cago, J. & Oliveira, E.R. (Eds).** Accuracy estimates and adaptive refinements in finite element computations, pp. 22–41, John Wiley & Sons, New York, USA.

(Received 26 June 1990, revised 2 June 1992)

دراسة تأثير التقاسيم ونوع العناصر المحدَّدة المستخدمة في «سترودل» على الأخطاء الناتجة في تحليل المنشآت في الأبعاد الثلاثة

هاني أحمد الغزالي* و مساعد فاضل الحسيني
قسم الهندسة المدنية بجامعة الكويت
ص. ب. ٥٩٦٩، الصفاة ١٣٠٦٠، الكويت

خلاصة

كثيرا ما نلجأ إلى استخدام التحليل في الأبعاد الثلاثة عند تصميم الآلات والأجزاء الإنشائية الغليظة. وعند استخدام طريقة العناصر المحدَّدة في التحليل فإن أول خطوة هي اختيار شبكة العناصر المحددة الملائمة. هذه الدراسة تختص بتأثير تناسب أبعاد ونوع العنصر على دقة الحل الناجم. تم استخدام البرنامج المعروف بـ «سترودل» لإنجاز التحليل في الأبعاد الثلاثة، حيث تم استخدام أربعة عناصر محددة فقط من العناصر المتاح استخدامها في «سترودل». ولكي نقدر الأخطاء الناتجة عن تطبيق طريقة العناصر المحددة تم اختيار ثلاث حالات لها حل معروف ودقيق بواسطة طريقة نظرية المرونة.

تتركز الدراسة على الأعضاء الإنشائية الطويلة حيث يكون البعد الممتد على امتداد محور العضو أطول بدرجة ملحوظة من أبعاد مقطع العضو. وبالرغم من أن النتائج المستنبطة تخص فقط الحالات المدروسة، إلا أن الدراسة بوجه عام تعطي فكرة عن مدى الأخطاء التي قد تنجم عند عمل دراسة في الأبعاد الثلاثة للمنشآت المشابهة.

*العنوان الحالي: قسم الهندسة المدنية بكلية الهندسة، الفيوم، ج. م. ع.